

## Electronic Supplemental Information for

### **Enhancing Photodynamic Therapy Efficacy of Black Phosphorus Nanosheets by Covalently Grafting Fullerene C<sub>60</sub>**

*Yajuan Liu,<sup>a,†</sup> Daoming Zhu,<sup>b,†</sup> Xianjun Zhu,<sup>a</sup> Gaoke Cai,<sup>c</sup> Jianhua Wu,<sup>a</sup> Muqing Chen,<sup>a</sup> Pingwu Du,<sup>a</sup> Yongshun Chen,<sup>c,\*</sup> Wei Liu,<sup>b,\*</sup> and Shangfeng Yang<sup>a,\*</sup>*

<sup>a</sup>Hefei National Laboratory for Physical Sciences at Microscale, CAS Key Laboratory of Materials for Energy Conversion, Anhui Laboratory of Advanced Photon Science and Technology, Department of Materials Science and Engineering, University of Science and Technology of China, Hefei 230026, China. E-mail: sfyang@ustc.edu.cn.

<sup>b</sup>Key Laboratory of Artificial Micro- and Nano-Structures of Ministry of Education, School of Physics and Technology, Wuhan University, Wuhan 430072, China. E-mail: wliu@whu.edu.cn.

<sup>c</sup>Department of Clinical Oncology, Renmin Hospital of Wuhan University, Wuhan 430072, China. E-mail: yongshun2007@163.com

†These authors contributed equally to this work.

## Contents

- S1. TEM images of the BP-C<sub>60</sub> hybrid, BP-BM, C<sub>60</sub>-BM and C<sub>60</sub>.**
- S2. AFM images and thickness distributions of the BP-C<sub>60</sub> hybrid and BP-BM.**
- S3. Degradation rates of the BP-C<sub>60</sub> hybrid and pristine BP-BM dispersed in serum, PBS and water with different times.**
- S4. Time-dependent fluorescence spectra of the BP-C<sub>60</sub> hybrid with terephthalic acid.**
- S5. Histopathologic examinations of the tissues including heart, liver, spleen, lung, and kidney from BALB/c mice for 14 d.**
- S6. The mechanism of the significantly enhanced PDT efficacy of the BP-C<sub>60</sub> hybrid.**

**S1. TEM images of the BP-C<sub>60</sub> hybrid, BP-BM, C<sub>60</sub>-BM and C<sub>60</sub>.**

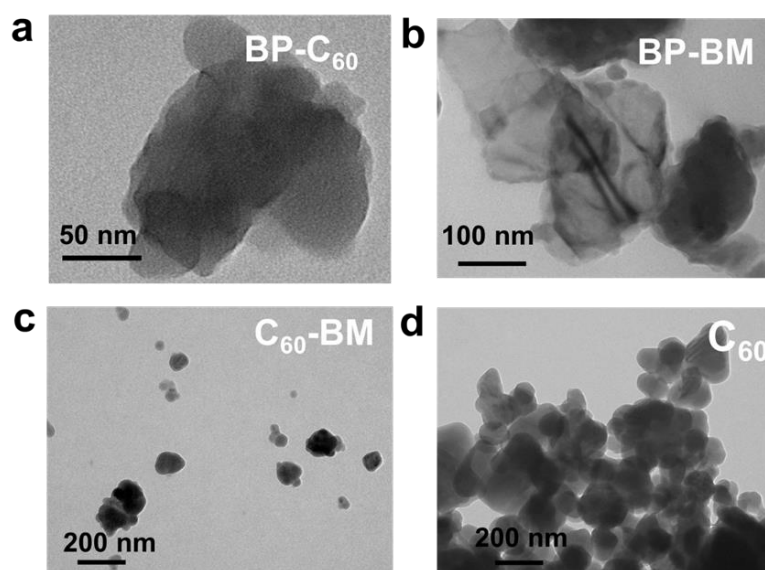


**Figure S1.** TEM images of BP-C<sub>60</sub> (a), BP-BM (b), C<sub>60</sub>-BM (c), and pristine C<sub>60</sub> (d).

**S2. AFM images and thickness distributions of the BP-C<sub>60</sub> hybrid and BP-BM.**

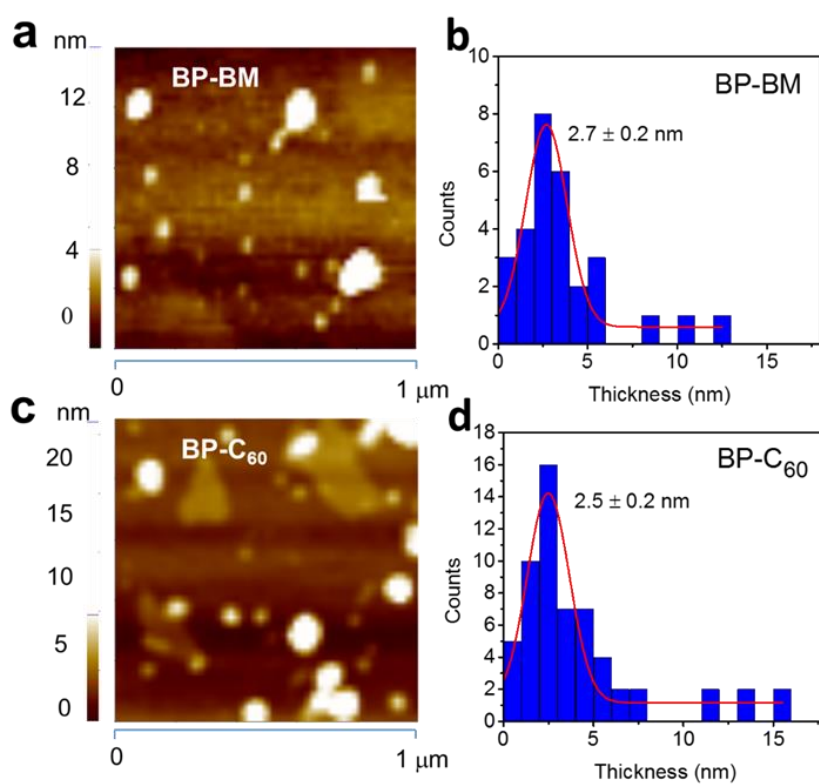


**Figure S2.** High-magnification AFM images (a, c) and the thickness distribution (b, d) of BP-BM and the BP-C<sub>60</sub> hybrid. Copied from ref. [S1]

**S3. Degradation rates of the BP-C<sub>60</sub> hybrid and pristine BP-BM dispersed in serum, PBS and water with different times.**

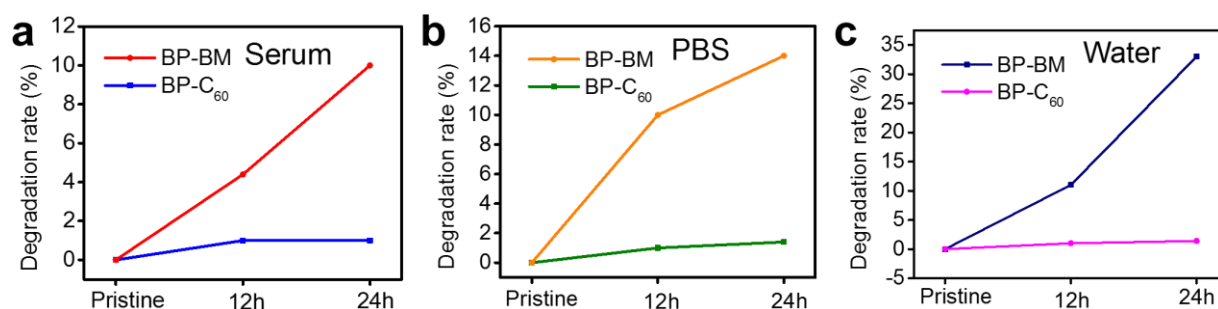


**Figure S3.** Degradation rate ( $1-A/A_0$ ) of the pristine BP-BM and BP-C<sub>60</sub> dispersed in serum (a), PBS (b) and Water (c) with different times.

**S4. Time-dependent fluorescence spectra of the BP-C<sub>60</sub> hybrid with terephthalic acid.**

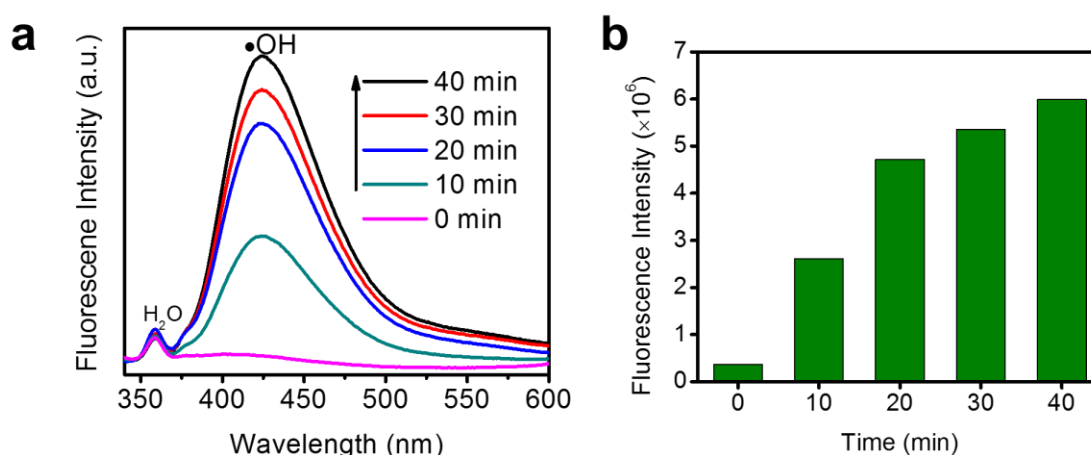


**Figure S4.** (a) Time-dependent fluorescence spectra of the BP-C<sub>60</sub> hybrid with terephthalic acid as scavenger of  $\cdot\text{OH}$  radicals. (b) Change of fluorescence intensity at 425 nm of the BP-C<sub>60</sub> hybrid with different times.

**S5. Histopathologic examinations of the tissues including heart, liver, spleen, lung, and kidney from BALB/c mice for 14 d.**

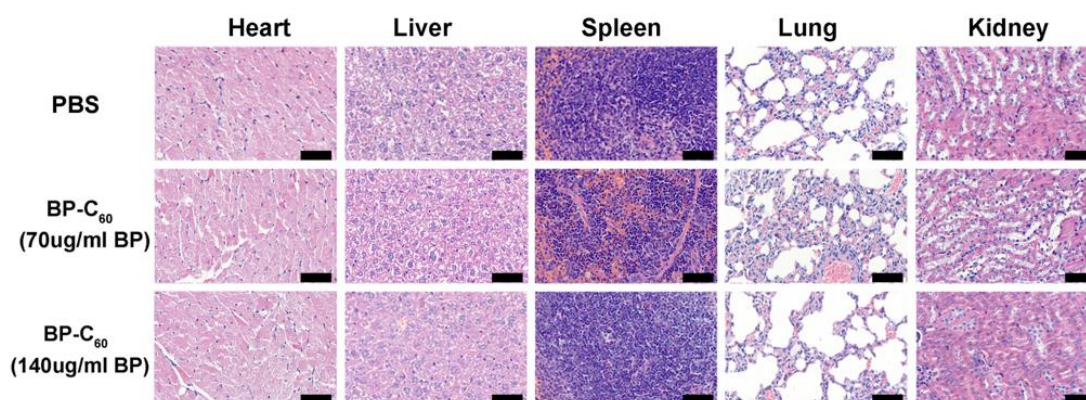


**Figure S5.** Histopathologic examination of the tissues including heart, liver, spleen, lung, and kidney from BALB/c mice by intravenous injection treatment of the BP-C<sub>60</sub> hybrid for 14 d.

Scale bar = 100  $\mu$ m

**S6. The mechanism of the significantly enhanced PDT efficacy of the BP-C<sub>60</sub> hybrid.**

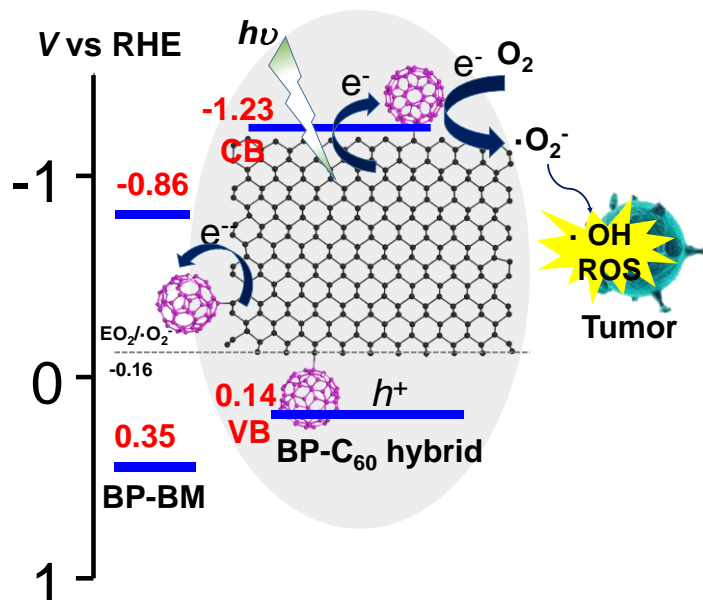


**Figure S6.** A schematic illustration showing the mechanism of the PDT efficacy of the BP-C<sub>60</sub> hybrid.

***References:***

S1. X. J. Zhu, T. M. Zhang, D. C. Jiang, H. L. Duan, Z. J. Sun, M. M. Zhang, H. C. Jin, R. N. Guan, Y. J. Liu, M. Q. Chen, H. X. Ji, P. W. Du, W. S. Yan, S. Q. Wei, Y. L. Lu and S. F. Yang, *Nat. Commun.*, 2018, **9**, 4177.